

# Substituent Effects of Pyridine-amine Nickel Catalyst Precursors on Ethylene Polymerization

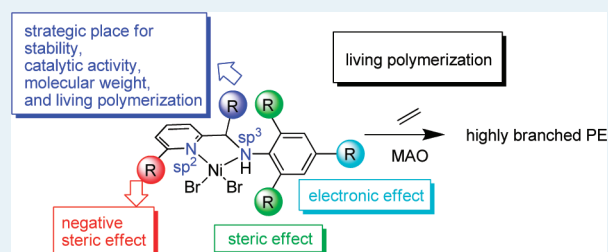
Shaobo Zai,<sup>†</sup> Haiyang Gao,<sup>\*,†,‡</sup> Zengfang Huang,<sup>†</sup> Haibin Hu,<sup>†</sup> Han Wu,<sup>†</sup> and Qing Wu<sup>\*,†,‡</sup>

<sup>†</sup>DSAPM Lab, Institute of Polymer Science, <sup>‡</sup>PCFM Lab, School of Chemistry and Chemical Engineering, Sun Yat-Sen University, Guangzhou, 510275, China

## Supporting Information

**ABSTRACT:** A series of pyridine-amine nickel complexes with various substituents were synthesized and used to evaluate substituent effects of catalyst precursors on the reactivity of ethylene polymerization. Substituent effects, including the steric effect of the pyridine moiety, steric effect of the bridge carbon, and steric and electronic effects of the amine moiety, were investigated systematically. Introduction of bulky aryls onto the pyridine moiety on amine pyridine nickel leads to a significant decrease in the activity and molecular weight of polyethylene, whereas an increase in bulk of substituents on the bridge carbon causes an increase in the polymerization activity and molecular weight of polyethylene. For the amine moiety, increasing the steric hindrance results in decreasing activity and affords a higher molecular weight polyethylene with a narrower polydispersity, and introduction of an electron-donating group on the amine moiety leads to formation of a high molecular weight polyethylene with enhanced activity. By optimizing ligand frameworks and reaction conditions, two bulky pyridine-amine nickel complexes are also developed successfully as catalyst precursors for living polymerization of ethylene.

**KEYWORDS:** pyridine-amine, nickel complex, ethylene, living polymerization



## INTRODUCTION

Transition metal catalysts offer a means to control structural variations in the molecular architecture of polyolefin materials.<sup>1–4</sup> Development of ligand synthesis and new metal–ligand combinations not only allows the fine-tuning of the chemical environment around the metal center but also advances the design of new polymeric materials. The combination of several main donor atoms such as N, O, P, S can offer various ligands coordinated to a late transition metal.<sup>1</sup> Among them, the ligands containing two nitrogen atoms, such as  $\alpha$ -diimine,<sup>5–7</sup>  $\beta$ -diimine,<sup>8,9</sup>  $\alpha$ -keto- $\beta$ -diimine,<sup>10,11</sup>  $\beta$ -diketiminato,<sup>12,13</sup> anilido-imine,<sup>14–18</sup> amidinate,<sup>19–21</sup> bis(imino)pyridine,<sup>22–25</sup> pyridine-imine,<sup>26</sup> pyridine-amide,<sup>27</sup> pyrrolide-imine,<sup>28,29</sup> and amide-imine,<sup>30,31</sup> have attracted considerable interest. Three types of combination fashions between transition metal and nitrogen atom are imine–metal ( $C=N \rightarrow Mt$ ) (including nitrogen heterocycles, such as pyridine), amide–metal ( $C-(R)N^- - Mt$ ), and amine–metal ( $C-(R^1)(R^2)N \rightarrow Mt$ ). Compared with the two former, the coordination of an amine and a late transition metal, which features  $sp^3$  nitrogen, has been rarely studied and applied to catalysis. A few examples have proved that this unique late transition metal–ligand combination is very useful for catalytic polymerization.<sup>32–36</sup> This prompted us to study the effect of the combination of an amine and a late transition metal on catalytic polymerization of olefin and to develop new olefin polymerization catalysts.

A type of nickel complex, supported by the pyridine-amine ligand, has recently been reported as an active catalyst precursor

for ethylene polymerization by our groups in a communication.<sup>37</sup> Living characteristics for ethylene polymerization can also be achieved using a bulky pyridine-amine nickel catalyst precursor by introducing a 2,4,6-trimethylphenyl group onto the bridge carbon between the amine and pyridine moieties. This provides a clear dependence between substituents on the pyridine-amine ligand framework and polymerization reactivity of ethylene. It is generally believed that the  $[N,N]$  bidentate pyridine-amine ligands with different hybrids potentially enable afford a distinct influence on the metal with regard to both polymer structure and reactivity control. Therefore, we herein synthesized a series of pyridine-amine nickel complexes with various substituents and study the substituent effects on ethylene polymerization in detail. The steric effect of the pyridine moiety, steric effect of the bridge carbon, and steric and electronic effects of the amine moiety were investigated systematically. On the basis of substituent effects of pyridine-amine nickel complexes on ethylene polymerization, we disclose a relationship between the pyridine-amine precursor structure and reactivity for ethylene polymerization. In addition, two pyridine-amine nickel complexes are also developed successfully as catalyst precursors for living polymerization of ethylene.

Received: November 15, 2011

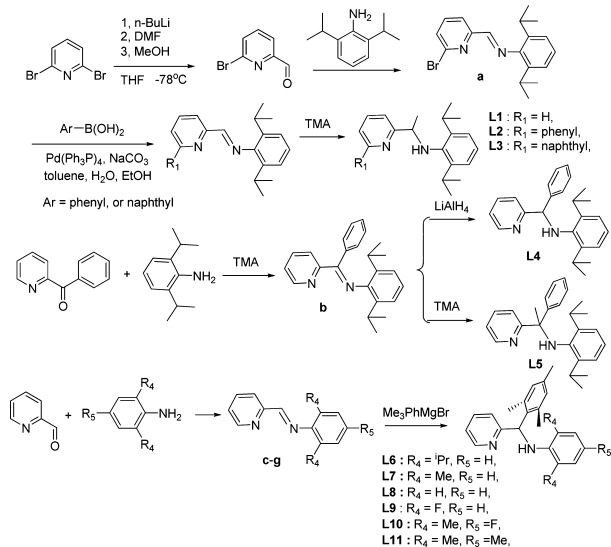
Revised: February 7, 2012

Published: February 8, 2012

## RESULTS AND DISCUSSION

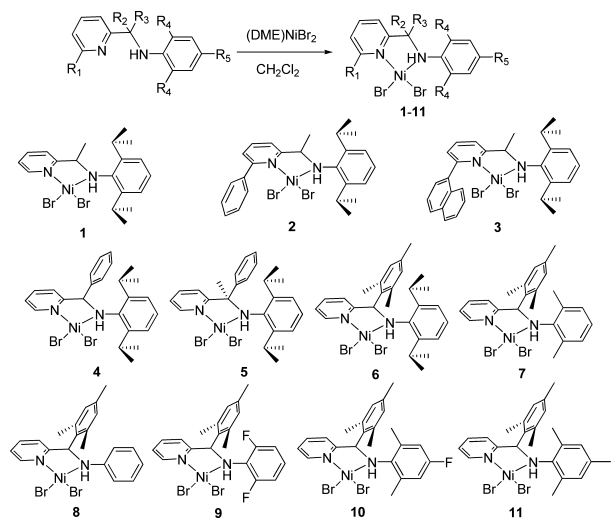
**Synthesis of Pyridine-Amine Ligands and Nickel(II) Complexes.** To enhance the steric effect of the pyridine moiety, phenyl and naphthyl were introduced onto the 6-position of pyridine via a Suzuki coupling reaction;<sup>38</sup> and ligands **L2** and **L3** can be obtained from 2,6-dibromopyridine in good yields. Substituents on the bridge carbon between the pyridine moiety and the amine moiety can be tuned by using different reduction agents, such as trimethylaluminum (TMA), LiAlH<sub>4</sub>, and Grignard reagent (2,4,6-Me<sub>3</sub>PhMgBr) for the imine group. Steric and electronic effects of the amine moiety can be readily varied by Schiff base condensation reactions from different substituted anilines. The general synthetic routes for the pyridineamine ligands **L1**–**L11** are shown in Scheme 1.

Scheme 1. Synthesis Routes of Pyridine-Amine Ligands



The corresponding nickel complexes **1**–**11** were obtained by the addition of ligands to a stirring suspension of (DME)NiBr<sub>2</sub> in CH<sub>2</sub>Cl<sub>2</sub>. Scheme 2 lists structures of pyridine-amine nickel

Scheme 2. Synthesis of Pyridine-amine Nickel Complexes 1–11



complexes **1**–**11**. The obtained ligands were fully characterized by NMR and elemental analyses, and the corresponding nickel

complexes were characterized by elemental analyses and MS (see the Supporting Information).

**Crystal Structure.** We have previously reported single-crystal X-ray diffraction data of complexes **1** and **6**. Single crystals **4** and **5** were herein also obtained from dichloromethane solutions layered with hexane. Like complex **1**, complex **4** exists as a bimolecular structure bridging by Br atoms (Figure 1).<sup>37</sup> The phenyl on the bridge carbon lies out of the

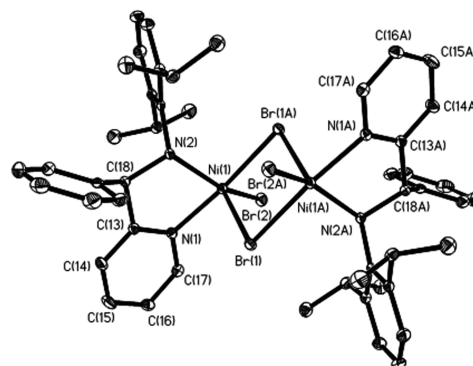


**Figure 1.** Molecular structure of complex **4** with hydrogen atoms omitted. Selected bond distances (Å) and angles (°): Br(1)–Ni(1) 2.5149(5), Br(2)–Ni(1) 2.4018(5), Ni(1)–N(1) 2.039(2), Ni(1)–N(2) 2.115(2), N(1)–Ni(1)–N(2) 81.56(9), N(1)–Ni(1)–Br(2) 99.00(6), N(2)–Ni(1)–Br(2) 150.13(6), N(1)–Ni(1)–Br(1) 86.20(6), N(2)–Ni(1)–Br(1) 99.06(6), Br(2)–Ni(1)–Br(1) 110.793(17).

one side of the slightly distorted chelate ring, showing a steric effect on the metal center. The amine moiety swings to another side of the chelate ring due to the distorted tetrahedral configuration of the nitrogen on the amine and is almost completely perpendicular.

Complex **5** containing a coordinated H<sub>2</sub>O was generated because of a reaction with moisture during crystallization. As shown in Figure 2, methyl and phenyl substituents on the

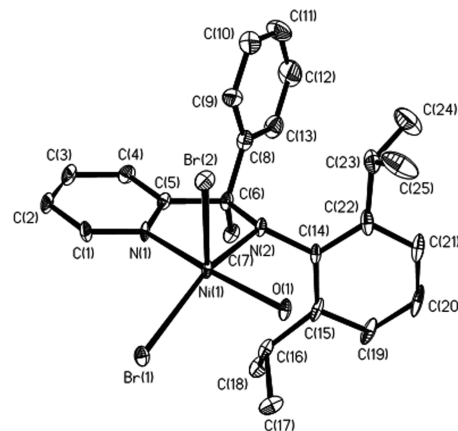


**Figure 2.** Molecular structure of **5** containing a molecule of H<sub>2</sub>O with hydrogen atoms and two CH<sub>2</sub>Cl<sub>2</sub> omitted. Selected bond distances (Å) and angles (°): Ni(1)–N(1) 2.027(5), Ni(1)–N(2) 2.107(6), Ni(1)–Br(1) 2.4477(12), Ni(1)–Br(2) 2.4658(12), N(1)–Ni(1)–N(2) 80.2(2), N(1)–Ni(1)–Br(1) 97.01(17), N(1)–Ni(1)–Br(2) 93.01(17), N(2)–Ni(1)–Br(2) 96.70(18), N(2)–Ni(1)–Br(1) 155.03(18), Br(2)–Ni(1)–Br(1) 108.24(4).

bridge carbon ((Me)PhCNH) are oriented toward two sides of the axial direction of the chelate ring, showing axially steric

blocks at the metal sites. The amine moiety swings to the side of the methyl on the bridge carbon, and the isopropyl groups on the aryl are almost completely perpendicular to the five-membered chelate ring. It is obvious that complex **5** exhibits more effective steric blocks at the axial sites than **4**, and introduction of another methyl on the bridge carbon can more effectively block the axial sites of the nickel metal.

It is interesting to note that all of the pyridine-amine nickel complexes are stable in the solid state, but solutions of nickel complexes in organic solvent exhibit different stabilities. A basic trend is that nickel complexes bearing bulky pyridine-amine ligands are more stable in solution. For example, a solution of bulky nickel complex **6** with 2,4,6-trimethylphenyl on the bridge carbon in  $\text{CH}_2\text{Cl}_2$  can exist for a long time (at least 7 days) at room temperature under  $\text{N}_2$  atmosphere. However, the solution color of nickel complex **1** with methyl on the bridge carbon slowly changed from brown to green under the same conditions, suggesting decomposition of **1** and appearance of a new nickel complex. A single crystal was obtained by careful treatment of the green solution and slow evaporation. Single crystal X-ray diffraction data confirmed that the new green nickel complex  $(\text{L}_1)_2\text{NiBr}_2$  is composed of two chelate ligands **L1**, nickel metal, and two Br atoms (Figure 3).  $(\text{L}_1)_2\text{NiBr}_2$

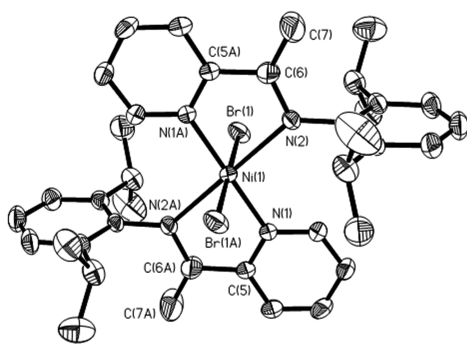
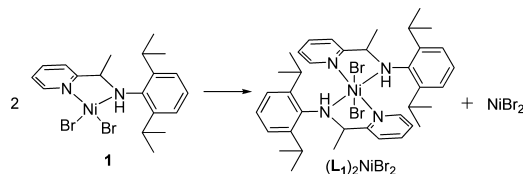


**Figure 3.** Molecular structure of  $(\text{L}_1)_2\text{NiBr}_2$  with hydrogen atoms omitted. Selected bond distances (Å) and angles ( $^\circ$ ): Br(1)–Ni(1) 2.5492(5), Ni(1)–N(1) 2.020(3), Ni(1)–N(2A) 2.348(3), N(1)–Ni(1)–N(2) 103.58(10), N(1)–Ni(1)–N(2A) 76.42(10), N(1)–Ni(1)–Br(1) 89.15(7), N(1A)–Ni(1)–Br(1) 90.85(7), N(2)–Ni(1)–Br(1) 90.13(9), N(2A)–Ni(1)–Br(1) 89.87(9).

adopts a six-coordinate environment around the nickel atom, where the two ligands act as bidentate  $N,N$  chelators, which is distinctive from the previously reported bimolecular structure of **1** bridging by Br atoms.<sup>37</sup> Scheme 3 depicts the pathway of

### Scheme 3. The Pathway of Decomposition of **1** and Formation of $(\text{L}_1)_2\text{NiBr}_2$



the decomposition of **1** and formation of  $(\text{L}_1)_2\text{NiBr}_2$ . A molecule of pyridine-amine nickel complex **1** can abstract the ligand of another molecule to produce the more stable  $(\text{L}_1)_2\text{NiBr}_2$  and  $\text{NiBr}_2$ . This fragmentation pattern with a halide loss has been observed to occur for pyridine-imine nickel compounds.<sup>39</sup>

Therefore, bulky steric hindrance is favorable for stability of the pyridine-amine complexes with a monoligand in solution,<sup>27</sup> which is anticipated to effectively keep the nickel active center stable in ethylene polymerization.

**Ethylene Polymerization.** To disclose the relationship between the structure and reactivity of ethylene polymerization, pyridine-amine complexes **1–11** were used as catalyst precursors for ethylene polymerization at atmospheric pressure (1.2 atm). Ethylene polymerizations were initiated by 800 equiv of MAO and lasted for 1 h at 0  $^\circ\text{C}$ . The detailed results are summarized in Table 1.

**Table 1.** Results of Ethylene Polymerization Catalyzed by Pyridine-amine Nickel **1–11**/MAO<sup>a</sup>

entry	precursor	yield (g)	activity <sup>b</sup>	$M_n^c$ (kg/mol)	PDI <sup>c</sup>	branches/ 1000 C <sup>d</sup>
1	<b>1</b>	0.192	9.6	1.3	1.98	93
2	<b>2</b>	oligomers				
3	<b>3</b>	oligomers				
4	<b>4</b>	0.231	11.6	5.0	1.83	66
5	<b>5</b>	0.335	16.8	6.3	1.39	69
6	<b>6</b>	0.438	21.9	17.5	1.27	67
7	<b>7</b>	0.763	38.2	15.1	1.38	98
8	<b>8</b>	traces/ oligomers				
9	<b>9</b>	0.088	4.4	1.4	1.97	64
10	<b>10</b>	0.484	24.2	13.5	1.57	92
11	<b>11</b>	1.382	69.1	23.8	1.34	107

<sup>a</sup>Polymerization conditions: 20  $\mu\text{mol}$  of nickel, 800 equiv of MAO, 1.2 atm ethylene pressure, 0  $^\circ\text{C}$  for 1h, 40 mL of toluene. <sup>b</sup>In units of kilograms of PE  $(\text{mol Ni})^{-1} \text{h}^{-1}$ , activity is calculated by the weight of the isolated solid polymer. <sup>c</sup>Determined by gel permeation chromatography (GPC) in 1,2,4-trichlorobenzene at 135  $^\circ\text{C}$  against linear polyethylene standards. <sup>d</sup>Branches per 1000 C atoms determined by  $^1\text{H}$  NMR spectroscopy.

The previous literature has reported that an axially steric block of late transition metal catalysts plays a crucial role in retarding chain transfer and improving catalytic activity.<sup>5–7,40</sup> In view of less axially steric effect of the pyridine moiety on the pyridine-amine nickel, **2** with phenyl and **3** with naphthyl on the 6-position of pyridine were synthesized and used to evaluate the steric effect of the pyridine moiety on ethylene polymerization. The results of ethylene polymerization in Table 1 show that only oligomers (no solid products) can be obtained for **2**/MAO and **3**/MAO catalytic systems at atmosphere pressure (entries 2, 3). Even under 20 atm pressure of ethylene, traces of solid PEs were obtained with both catalytic systems.

Comparison of entries 1, 2, and 3 in Table 1 demonstrates that introduction of bulky aryls on the pyridine moiety leads to a significant decrease in the activity and molecular weight of products for ethylene polymerization. This result is contrary to the observation using salicylaldimino nickel catalyst<sup>40</sup> but similar to that obtained with pyridine-imine nickel catalyst.<sup>41,42</sup> Grubbs previously reported that introduction of the bulky phenyl or anthracene group onto the salicylaldimino ligand can markedly enhance the catalytic activity of nickel catalysts for ethylene polymerization.<sup>40</sup> However, decreasing activity was also observed by the introduction of a methyl group onto the 6-position of the pyridine for pyridine-imine nickel catalyst,<sup>41,42</sup> and only oligomers can be obtained when substituting the bulky 2, 6-dimethylphenyl onto the pyridine moiety.<sup>43</sup> Reduction of the activity and molecular weight of the obtained

product were observed for the pyridine-amine catalyst by introduction of aryl groups onto the 6-position of the pyridine moiety, which may be attributed to the weak axially steric effect of the pyridine plane and the reducing basicity of the pyridine ring.<sup>41,42</sup>

On the basis of the negative steric effect of the pyridine moiety, we further investigated the steric effect of the substituent on the bridge carbon using nickel complexes with the chelating pyridine moiety without a substituent. Ethylene polymerizations were carried out using **1**/MAO, **4**/MAO, **5**/MAO, and **6**/MAO to evaluate the substituent effect of the bridge carbon under the same conditions. When phenyl was introduced onto the bridge carbon instead of methyl, an increase in the catalytic activity and molecular weight of the polyethylene (PE) was observed. An obvious increase in the molecular weight of the polyethylene in a fold of ~4 can be explained as increasing the steric bulk from methyl to phenyl, which can retard the chain transfer reaction. When the bulky 2,4,6-trimethylphenyl was introduced, both the catalytic activity and molecular weight of the polymer significantly increased. Compound **6** with a 2,4,6-trimethylphenyl on the bridge carbon exhibits a catalytic activity over twice higher than **1** with methyl, and the molecular weight of the PE obtained by **6**/MAO is higher than that of PE with **1**/MAO by a factor of ~13.5. In addition, reducing the PDI value from 1.98 to 1.27 is consistent with our previous observation.<sup>37</sup> These results further support that bulky substituents on the bridge carbon play an important role in the catalytic activity and molecular weight of the products. As compared with complex **4**, nickel complex **5** with phenyl and methyl substituents activated by MAO exhibited the higher activity and afforded the higher molecular weight polymer with a narrower polydispersion (PDI = 1.39). This result provides a demonstration that disubstituents on the bridge carbon can also have a similar role for 2,4,6-trimethylphenyl and effectively block two sides of the axial space of the nickel metal.

In view of the positive steric effect of the substituent on the bridge carbon, the 2,4,6-trimethylphenyl moiety was thus retained on the pyridine-amine ligand framework to further study the steric and electronic effects of the amine moiety on ethylene polymerization. First, pyridine-amine nickel complexes **6**, **7**, **8** with different 2,6-disubstituents were used to study the steric effects of the amine moiety (entries 6, 7, 8). Reducing the steric hindrance of the amine moiety by substituting *o*-methyl groups for *o*-isopropyl groups results in an increase in the polymerization activity, but a decreasing-molecular-weight polymer with a broadened polydispersity. Lack of substituents on an *N*-aryl leads to a remarkable drop in the molecular weight of polyethylene, and oligomers/traces of solid polymer are obtained. This result illuminates that bulky steric hindrance of the amine moiety can also effectively prohibit the chain transfer reaction, which agrees with previous observations using pyridine-imine nickel<sup>41,42</sup> and  $\alpha$ -diimine nickel catalytic systems.<sup>7</sup>

In addition, we attempted to evaluate the electronic effect of the ortho position of the aryl ring by introducing two fluorine groups. The bi-F substituted complex **9** after activation with MAO can afford a small amount of isolated solid polymer product with a low molecular weight (entry 9). Comparison of activities between **8** and **9** shows a slight increase in the yield of the polymer by introducing F onto the ortho position of the aryl ring instead of H. Part of the explanation may be an electronic effect because of the electron-withdrawing nature of the F groups, but the increasing sizes of F vs H groups suggests that

a steric effect should be responsible for slightly increasing the molecular weight. In fact, a larger consumption of ethylene can be observed using **8**/MAO, which further confirmed that introduction of electron-withdrawing onto the para position of leads to a decrease in the turnover frequency.

Considering the high activity of pyridine-amine nickel **7** with 2,6-dimethylphenyl, we further synthesized another two pyridine-amine nickel analogues, **10** and **11**, and studied the electronic effect of a para substituent on the amine moiety. Comparison of entries **7** vs **10** demonstrates that introduction of F onto the para position of the aryl leads to a decrease in the activity and molecular weight of the polyethylene, which further supports that the influence of F groups on the ortho position of the aryl on molecular weight comes from steric hindrance. When methyl is used instead of F, an increasing activity and molecular weight of the polyethylene can be observed. Increasing the activity by introduction of a methyl group onto the para position of the aryl not only arises from the electron-donating effect of methyl, but also may be attributed to an increasing axially steric block because of the tetrahedral configuration of nitrogen on the amine (see the Crystal Structure Section).

The branching structures of the polyethylenes produced by pyridine-amine nickel catalysts were determined by <sup>1</sup>H NMR and are listed in Table 1. Generally, highly branched products can be obtained as a result of the occurrence of the chain walking process during ethylene polymerization. Even at 0 °C, the shortest branch-on-branch structure generated via chain walking through tertiary carbons can be seen from the methyl and ethyl resonances centered at 19.44 and 11.72 ppm, respectively (Figure 4).<sup>7</sup>

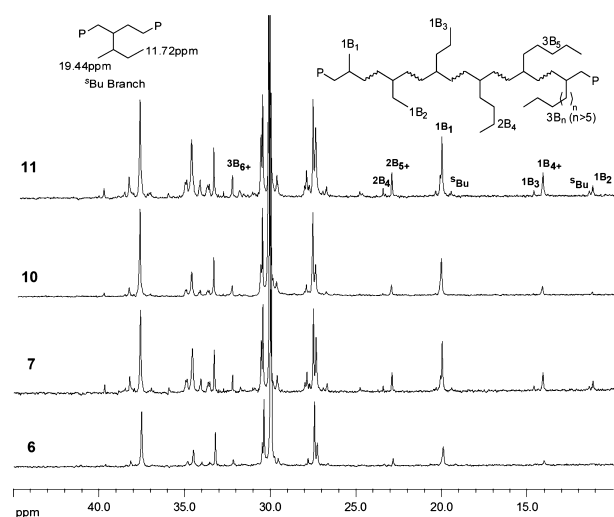


**Figure 4.** <sup>13</sup>C NMR spectra of polyethylene samples synthesized by **6**/MAO, **7**/MAO, **10**/MAO, and **11**/MAO at 0 °C.

The catalyst precursor structure has an influence on the branching structure of the PEs. For the influence of the substituent on the bridge carbon, a general tendency is that introduction of bulky substituents onto a bridge carbon leads to a decrease in the total branch density. Steric and electronic effects of the amine moiety on the branching structure of polyethylenes were herein investigated in detail. <sup>13</sup>C NMR experiments were conducted to detect the branching distributions of the polyethylenes (Figure 4), and detailed branching distributions of the polyethylenes obtained by various catalysts are listed in

Table 2. Branching Distributions of Polyethylenes Obtained with Complexes 6/MAO, 7/MAO, 10/MAO, and 11/MAO

entry	Ni	branched chain/1000 C (relative content)						branches/1000 C
		Me	Et	Pr	Bu	Pe	Lg	
6	6	55.7 (73.3%)	6.5 (8.6%)	3.6 (4.8%)	3.9 (5.1%)	0 (0%)	6.3 (8.2%)	76
7	7	67.0 (63.8%)	8.6 (8.2%)	3.7 (3.5%)	4.1 (3.9%)	3.4 (3.2%)	17.9 (17.4%)	105
10	10	62.4 (63.7%)	11.5 (11.7%)	3.9 (4.0%)	3.6 (3.7%)	2.0 (2.0%)	14.7 (14.9%)	98
11	11	72.5 (60.9%)	10.4 (8.7%)	5.8 (4.9%)	6.0 (5.0%)	4.3 (3.6%)	20.1 (16.9%)	119

Table 3. Results of Ethylene Polymerization Catalyzed by 5/MAO and 11/MAO at Various Temperatures<sup>a</sup>

entry	precursor	temp. (°C)	yield (g)	activity <sup>b</sup>	$M_n^c$ (kg/mol)	PDI <sup>c</sup>	branches/1000 C <sup>d</sup>
11	5	-20	0.067	3.4	4.5	1.15	62
12	5	-10	0.110	5.5	8.3	1.24	64
5	5	0	0.335	16.8	6.3	1.39	69
13	5	20	0.484	24.2	5.1	1.61	87
14	5	40	0.231	11.6	3.8	1.79	106
15	11	-20	0.632	31.6	33.0	1.17	68
16	11	-10	0.950	47.5	31.5	1.27	94
10	11	0	1.382	69.1	23.8	1.34	107
17	11	20	1.412	70.6	23.4	1.59	113
18	11	40	1.076	53.8	14.2	1.87	128

<sup>a</sup>Polymerization conditions: 20  $\mu$ mol of nickel, 800 equiv of MAO, 1.2 atm ethylene pressure, 1 h, 40 mL of toluene. <sup>b</sup>In units of kilograms of PE (mol Ni)<sup>-1</sup> h<sup>-1</sup>, activity is calculated by the weight of isolated solid polymer. <sup>c</sup>Determined by gel permeation chromatography (GPC) in 1,2,4-trichlorobenzene at 135 °C against linear polyethylene standards. <sup>d</sup>Branches per 1000 C atoms determined by <sup>1</sup>H NMR spectroscopy.

Table 2. The values of the branching density determined by <sup>13</sup>C NMR are reasonably larger than those determined by <sup>1</sup>H NMR.<sup>44</sup> Unlike a pyridine-imine nickel catalyst,<sup>41,42</sup> a contrasting trend is that reducing the steric bulk on the 2,6-positions of an aryl from isopropyl to methyl leads to a significant increase in the total branching density from 76 to 105 per 1000 carbon atoms. Compared with 7, electron-deficient catalyst 10 with F on the para position of the amine moiety afforded the PE with a lower branching density, whereas electron-rich catalyst 11 with a methyl afforded the PE with a higher branching density. These data suggest that reducing the steric hindrance and introduction of an electron-donating group for the amine moiety are favorable for the occurrence of chain walking during ethylene polymerization. This provides a fundamental approach for a pyridine-amine nickel catalyst to control the polyethylene branching structure.

In our earlier communication, we found that the polymerization temperature can affect the catalytic activity, polymer microstructure, and living polymerization behavior using 6/MAO.<sup>37</sup> On the basis of the above evaluation, pyridine-amine nickel precursors 5 and 11 were herein chosen to study the influence of the reaction temperature on ethylene polymerization. Table 3 summarized the polymerization results in the temperature range from -20 to 40 °C. The observed basic trend is that the catalytic activities of both catalytic systems reach the maximum values at 20 °C and then slightly decrease with elevated temperature.

Molecular weight distributions (PDI) received more attention to study the relationship between the precursor structure and living polymerization of ethylene. It is worth noting that molecular weight distributions of the polymer become narrower with decreasing temperature. PDI values of 1.15 and 1.17 can be achieved at -20 °C using 5/MAO and 11/MAO,

respectively. Therefore, living polymerizations of ethylene were performed at -20 °C using 5/MAO and 11/MAO. Figure 5b

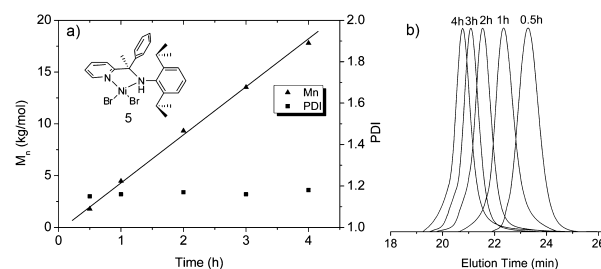
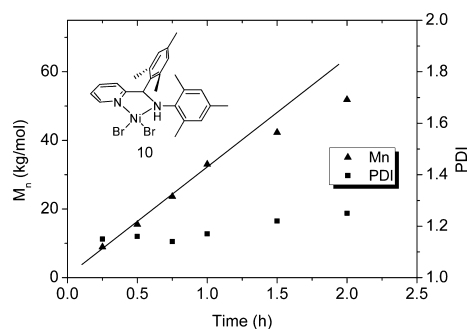


Figure 5. (a) Plots of  $M_n$  (▲) and  $M_w/M_n$  (PDI) (■) as a function of polymerization time using 5/MAO at -20 °C (polymerization conditions: 1.2 atm, 20  $\mu$ mol of Ni, 800 equiv of MAO, 40 mL of toluene). (b) GPC traces at different times.

shows symmetric GPC traces of the polymers obtained using 5/MAO at different polymerization times, which shift to the higher molecular weight region with the prolonged polymerization time. Plots of number-average molecular weight ( $M_n$ ) and  $M_w/M_n$  as a function of polymerization time (Figure 5a) also illustrate that  $M_n$  grows linearly with the polymerization time, and  $M_w/M_n$  (PDI) values are below 1.2. Because the branching density and type are nonuniform in each chain of branched PEs with the same molecular weight, different hydrodynamic volumes of a branched PE chain lead to a slightly broadened polydispersity.<sup>45</sup> In addition, ethylene consumption with 5/MAO measured by an ethylene flow rate meter over a period of 4 h at -20 °C stays constant after a very short initiation stage during the polymerization process. This result also strongly supports that the active species is stable and long-lived under the adopted conditions. Therefore, ethylene

polymerizations using **5**/MAO at  $-20\text{ }^{\circ}\text{C}$  proceed in a living manner within 4 h.

In addition, a good linear relationship between  $M_n$  and polymerization time is also observed over a period of 1 h for **11**/MAO, and PDI values are below 1.2 (Figure 6). With a



**Figure 6.** Plots of  $M_n$  (▲) and  $M_w/M_n$  (PDI) (■) as a function of polymerization time using **11**/MAO at  $-20\text{ }^{\circ}\text{C}$  (polymerization conditions: 1.2 atm, 20  $\mu\text{mol}$  of Ni, 800 equiv of MAO, 40 mL of toluene).

prolonged polymerization time, the slope begins to decrease, and the molecular weight distribution becomes broad, reaching 1.24 at 2 h. A broadening molecular weight distribution after 2 h may arise from precipitation of high molecular weight polymers ( $M_n = 52\ 000$ ) at low temperature and embedment of nickel species.<sup>46,47</sup> Therefore, it is safely concluded that the living polymerization of ethylene can proceed with **11**/MAO at  $-20\text{ }^{\circ}\text{C}$  within 1 h. The living catalytic polymerization behavior of pyridine-amine nickel **11** not only arises from an axially steric block on the bridge carbon, but also may be attributed to effective steric hindrance of the amine moiety as a result of the tetrahedral configuration of nitrogen on the amine, which can retard chain transfer. To the best of our knowledge, this type of pyridine-amine nickel is one of rare late transition metal catalytic systems for living polymerization of ethylene.<sup>10,11,48–51</sup> Living polymerization of ethylene provides viable access to precise synthesis of monodisperse PE and corresponding block copolymers.

Living polymerization of ethylene proved that a single-site, nickel-based active species can be formed when pyridine-amine nickel complexes were activated by MAO. It is known that the amine group (C–(R)NH) can be deprotonated by a strong base, such as BuLi or KH, to produce the amide (C–(R)N<sup>–</sup>) group, and an amide–metal combination arrangement also generally occurs.<sup>27,52,53</sup> Herein, a crucial problem for active species for ethylene polymerization is whether cation pyridine-amine nickel ([Py–CNRH]Ni<sup>+</sup>P, P is polymer chain) or neutral pyridine-amide nickel ([Py–CNR]NiP) when a hydrogen on the amine group is removed by activator MAO. We have previously synthesized well-defined pyridine-amide nickel complexes without a substituent on the bridge carbon and studied their polymerization behavior for ethylene.<sup>27</sup> In the presence of MAO, pyridine-amide nickel complexes catalyze ethylene polymerization to afford a coexisting product of a solid polymer and liquid oligomers, which may be attributed to different catalytic species yielded from isomerization equilibrium by the rotation of the amide–aryl bond.

In addition, much lower branched polyethylene (<10/1000 C) were produced by a pyridine-amide nickel catalyst<sup>27</sup> than pyridine-amine nickel catalyst (60–70/1000 C) at  $-20\text{ }^{\circ}\text{C}$ .

The above comparison of ethylene polymerization strongly confirmed two distinct active species between pyridine-amide nickel/MAO and pyridine-amine nickel/MAO. Therefore, it is reasonably concluded that an active species for ethylene polymerization is the cation pyridine-amine nickel ([Py–CNRH]–Ni<sup>+</sup>P), and our conclusion is also supported by the cation imine–amine nickel species for ethylene polymerization presented by Chen.<sup>33,34</sup> One explanation is that a hydrogen on an amine group can be avoided to deprotonate by MAO because of bulky steric hindrance.

## CONCLUSIONS

A series of novel nickel complexes chelating pyridine-amine ligands were synthesized. The variation of the pyridine-amine framework has a decisive influence on ethylene polymerization. Introduction of bulky aryls on the pyridine moiety on amine-pyridine nickel leads to a significant decrease in the activity and molecular weight of the polyethylene, whereas increasing the bulk of the substituents on the bridge carbon results in an increase in the polymerization activity and molecular weight of polyethylene. For an amine moiety, increasing the steric hindrance results in decreasing activity and affords high-molecular-weight polyethylene with a narrower polydispersity, and introduction of an electron-donating group on the amine moiety leads to the formation of high-molecular-weight polyethylene with an enhanced activity. The above shows that two coordinating functionalities (pyridine (sp<sup>2</sup>) and amine (sp<sup>3</sup>)) confer distinctive effects and reactivity controls on ethylene polymerization, and substituents on bridge carbon are located at a strategic place for the stability, activity, molecular weight of the polymer, and living polymerization of ethylene. By optimization of variations in pyridine-amine frameworks, a living polymerization of ethylene can be achieved using two new pyridine-amine nickel catalysts. This type of ethylene living polymerization catalyst will provide more choices to precise synthesis of monodisperse PE and corresponding block copolymers.

## EXPERIMENTAL SECTION

### General Procedure for Synthesis of Nickel Complexes.

A solution of the corresponding ligand in CH<sub>2</sub>Cl<sub>2</sub> (30 mL) and (DME)NiBr<sub>2</sub> was stirred under N<sub>2</sub> for 12 h. After filtration, the solution was evaporated to low volume in vacuum, and 20 mL of hexane was added. The mixture was stirred and filtered, and then the residual solid was obtained by washing with *n*-hexane. Drying in vacuum produced the desired nickel complexes. The nickel complexes were dissolved in a hot hexane/toluene solution and cooled in a freezer several days to afford the product as dark brown crystals. Characterizations of nickel complexes are shown in the Supporting Information. Crystal data and structure refinement for nickel complexes **4**, **5**·H<sub>2</sub>O and (L<sub>1</sub>)<sub>2</sub>NiBr<sub>2</sub> are shown in Table 4.

**Ethylene Polymerization.** In a typical procedure, a round-bottom Schlenk flask with stirring bar was heated 3 h to 150  $^{\circ}\text{C}$  under vacuum and then cooled to room temperature. The flask was pressurized to 1.5 atm of ethylene and vented three times. The appropriate MAO solid as cocatalyst and toluene were introduced into the glass reactor under 1.2 atm of ethylene. The system was maintained by continuously stirring for 5 min, and then a solution of the nickel complex in toluene was syringed into the well-stirred solution, and the total volume was kept at 40 mL. The ethylene pressure was kept constant at 1.2 atm (absolute pressure) by continuous feeding of gaseous ethylene

Table 4. Crystal Data and Structure Refinement for Complexes 4, 5·H<sub>2</sub>O and (L<sub>1</sub>)<sub>2</sub>NiBr<sub>2</sub>

	4	5·H <sub>2</sub> O	(L <sub>1</sub> ) <sub>2</sub> NiBr <sub>2</sub>
empirical formula	C <sub>48</sub> H <sub>56</sub> Br <sub>4</sub> N <sub>4</sub> Ni <sub>2</sub>	C <sub>27</sub> H <sub>35</sub> Br <sub>2</sub> Cl <sub>4</sub> N <sub>2</sub> NiO	C <sub>38</sub> H <sub>52</sub> Br <sub>2</sub> N <sub>4</sub> Ni
formula weight	1126.03	763.90	783.33
crystal system	monoclinic	monoclinic	monoclinic
space group	<i>P</i> 2 <sub>1</sub> / <i>n</i>	<i>P</i> 2(1)/ <i>c</i>	<i>P</i> 2(1)/ <i>c</i>
<i>a</i> (Å)	14.0495(19)	18.146(3)	11.7518(17)
<i>b</i> (Å)	9.9391(14)	12.048(2)	10.9119(16)
<i>c</i> (Å)	17.681(2)	18.386(3)	18.5929(19)
<i>α</i> (deg)	90	90	90
<i>β</i> (deg)	110.777(2)	119.140(3)	128.486(6)
<i>γ</i> (deg)	90	90	90
volume (Å <sup>3</sup> )	2308.4(5)	3511.0(10)	1866.3(4)
<i>Z</i>	2	4	2
<i>D</i> (calcd) (g/cm <sup>3</sup> )	1.620	1.445	1.394
<i>F</i> (000)	1136	1540	812
crystal size (mm)	0.50 × 0.40 × 0.20	0.30 × 0.20 × 0.20	0.48 × 0.46 × 0.24
<i>θ</i> range (deg)	1.60–27.09	2.11–26.10	2.21–27.05
index ranges	−18 ≤ <i>h</i> ≤ 10 −12 ≤ <i>k</i> ≤ 12 −22 ≤ <i>l</i> ≤ 22	20 ≤ <i>h</i> ≤ 22 −14 ≤ <i>k</i> ≤ 12 −22 ≤ <i>l</i> ≤ 19	−15 ≤ <i>h</i> ≤ 14 −13 ≤ <i>k</i> ≤ 13 −14 ≤ <i>l</i> ≤ 23
reflections collected/unique	12518/5015 ( <i>R</i> <sub>int</sub> = 0.0322)	17062/6864 ( <i>R</i> <sub>int</sub> = 0.0598)	10632/4058 ( <i>R</i> <sub>int</sub> = 0.0269)
data completeness	98.6%	98.5%	99.2%
transmission (max/min)	0.422/0.137	0.5711/0.4513	0.524/0.286
data/restraints/parameters	5015/0/267	6864/6/361	4058/15/217
goodness-of-fit on <i>F</i> <sup>2</sup>	1.056	1.115	1.023
final <i>R</i> indices [ <i>I</i> > 2σ( <i>I</i> )]	<i>R</i> <sub>1</sub> = 0.0289, w <i>R</i> <sub>2</sub> = 0.0634	<i>R</i> <sub>1</sub> = 0.0708, w <i>R</i> <sub>2</sub> = 0.1924	<i>R</i> <sub>1</sub> = 0.0381, w <i>R</i> <sub>2</sub> = 0.0898
<i>R</i> indices (all data)	<i>R</i> <sub>1</sub> = 0.0487, w <i>R</i> <sub>2</sub> = 0.0713	<i>R</i> <sub>1</sub> = 0.1110, w <i>R</i> <sub>2</sub> = 0.2198	<i>R</i> <sub>1</sub> = 0.0699, w <i>R</i> <sub>2</sub> = 0.1040
largest diff peak and hole (e Å <sup>−3</sup> )	0.510, −0.524	2.305, −1.079	0.699, −0.388

throughout the reaction. The low temperatures were controlled with a circulation cooler using ethanol as medium in the polymerization experiments. The polymerizations were terminated by the addition of 200 mL of acidic methanol (95:5 ethanol/HCl) after continuously stirring for an appropriate period. The resulting precipitated polymers were collected and treated by filtration, washing with methanol several times, and drying in vacuum at 50 °C to a constant weight. All polymerizations of ethylene were reproduced, and the yield and catalytic activity are average values.

## ASSOCIATED CONTENT

### Supporting Information

General experimental and characterization procedures, synthesis and characterization of ligands and nickel complexes, and crystallographic data. This material is available free of charge via the Internet at <http://pubs.acs.org>.

## AUTHOR INFORMATION

### Corresponding Author

\*Phone: +86-20-84113250. Fax: +86-20-84114033. E-mail: (H.G.) [gaohy@mail.sysu.edu.cn](mailto:gaohy@mail.sysu.edu.cn), (Q.W.) [ceswuq@mail.sysu.edu.cn](mailto:ceswuq@mail.sysu.edu.cn).

### Notes

The authors declare no competing financial interest.

## ACKNOWLEDGMENTS

Financial support from NSFC (Projects 20974125, 21174164, and 20734004) and the Fundamental Research Funds for the

Central Universities (Project 10lgpy10) is gratefully acknowledged.

## REFERENCES

- (1) Ittel, S. D.; Johnson, L. K.; Brookhart, M. *Chem. Rev.* **2000**, *100*, 1169–1203.
- (2) Mecking, S. *Coord. Chem. Rev.* **2000**, *203*, 325–351.
- (3) Coates, G. W.; Hustad, P. D.; Reinartz, S. *Angew. Chem., Int. Ed.* **2002**, *41*, 2236–2257.
- (4) Gibson, V. C.; Spitzmesser, S. K. *Chem. Rev.* **2003**, *103*, 283–315.
- (5) Johnson, L. K.; Killian, C. M.; Brookhart, M. *J. Am. Chem. Soc.* **1995**, *117*, 6414–6415.
- (6) Johnson, L. K.; Mecking, S.; Brookhart, M. *J. Am. Chem. Soc.* **1996**, *118*, 267–268.
- (7) Liu, F.; Hu, H.; Xu, Y.; Guo, L.; Zai, S.; Song, K.; Gao, H.; Zhang, L.; Zhu, F.; Wu, Q. *Macromolecules* **2009**, *42*, 7789–7796.
- (8) Feldman, J.; McClain, S. J.; Parthasarathy, A.; Marshall, W. J.; Calabrese, J. C.; Arthur, S. D. *Organometallics* **1997**, *16*, 1514–1516.
- (9) Zhang, J.; Ke, Z.; Bao, F.; Long, J.; Gao, H.; Zhu, F.; Wu, Q. *J. Mol. Catal. A: Chem.* **2006**, *249*, 31–39.
- (10) Azoulay, J. D.; Rojas, R. S.; Serrano, A. V.; Ohtaki, H.; Galland, G. B.; Bazan, G. C. *Angew. Chem., Int. Ed.* **2009**, *48*, 1089–1092.
- (11) Azoulay, J. D.; Schnerder, Y.; Galland, G. B.; Bazan, G. C. *Chem. Commun.* **2009**, 6177–6179.
- (12) Eckert, N. A.; Bones, E. M.; Lachicotte, R. J.; Holland, P. L. *Inorg. Chem.* **2003**, *42*, 1720–1725.
- (13) Zhang, J.; Gao, H.; Ke, Z.; Bao, F.; Zhu, F.; Wu, Q. *J. Mol. Catal. A: Chem.* **2005**, *231*, 27–34.
- (14) Gao, H.; Guo, W.; Bao, F.; Gui, G.; Zhang, J.; Zhu, F.; Wu, Q. *Organometallics* **2004**, *23*, 6273–6280.
- (15) Gao, H.; Zhang, J.; Chen, Y.; Zhu, F.; Wu, Q. *J. Mol. Catal. A: Chem.* **2005**, *240*, 178–185.

- (16) Gao, H.; Chen, Y.; Zhu, F.; Wu, Q. *J. Polym. Sci., Part A: Polym. Chem.* **2006**, *44*, 5237–5246.
- (17) Gao, H.; Ke, Z.; Pei, L.; Song, K.; Wu, Q. *Polymer* **2007**, *48*, 7249–7254.
- (18) Gao, H.; Pei, L.; Song, K.; Wu, Q. *Eur. Polym. J.* **2007**, *43*, 908–914.
- (19) Barker, J.; Kilner, M. *Coord. Chem. Rev.* **1994**, *133*, 219–300.
- (20) Coles, M. P. *J. Chem. Soc., Dalton Trans.* **2006**, 985–1001.
- (21) Liu, F.; Gao, H.; Song, K.; Zhao, Y.; Long, J.; Zhang, L.; Zhu, F.; Wu, Q. *Polyhedron* **2009**, *28*, 673–678.
- (22) Small, B. L.; Brookhart, M.; Bennett, A. M. *J. Am. Chem. Soc.* **1998**, *120*, 4049–4050.
- (23) Britovsek, G. J. P.; Gibson, V. C.; Kimberley, B. S.; Maddox, P. J.; McTavish, S. J.; Solan, G. A.; White, A. J. P.; Williams, D. J. *Chem. Commun.* **1998**, 849–850.
- (24) Britovsek, G. J. P.; Bruce, M.; Gibson, V. C.; Kimberley, B. S.; Maddox, P. J.; Mastroianni, S.; McTavish, S. J.; Redshaw, C.; Solan, G. A.; Strömberg, S.; White, A. J. P.; Williams, D. J. *J. Am. Chem. Soc.* **1999**, *121*, 8728–8740.
- (25) Guo, L.; Gao, H.; Zhang, L.; Zhu, F.; Wu, Q. *Organometallics* **2010**, *29*, 2118–2125.
- (26) Bianchini, C.; Giambastiani, G.; Luconi, L.; Meli, A. *Coord. Chem. Rev.* **2010**, *254*, 431–455.
- (27) Huang, Z.; Song, K.; Liu, F.; Long, J.; Hu, H.; Gao, H.; Wu, Q. *J. Polym. Sci., Part A: Polym. Chem.* **2008**, *46*, 1618–1628.
- (28) Li, Y.; Li, Y.; Li, X. *J. Organomet. Chem.* **2003**, *667*, 185–191.
- (29) Yoshida, Y.; Matsui, S.; Fujita, T. *J. Organomet. Chem.* **2005**, *690*, 4382–4397.
- (30) Froese, R. D. J.; Jazdzewski, B. A.; Klosin, J.; Kuhlman, R. L.; Theriault, C. N.; Welsh, D. M. *Organometallics* **2011**, *30*, 251–262.
- (31) Waele, P. D.; Jazdzewski, B. A.; Klosin, J.; Murray, R. E.; Theriault, C. N.; Vosejka, P. C. *Organometallics* **2007**, *26*, 3896–3899.
- (32) Britovsek, G. J. P.; Gibson, V. C.; Mastroianni, S.; Oakes, D. C. H.; Redshaw, C.; Solan, G. A.; White, A. J. P.; Williams, D. J. *Eur. J. Inorg. Chem.* **2001**, 431–437.
- (33) Yang, F.; Chen, Y.; Lin, Y.; Yu, K.; Liu, Y.; Wang, Y.; Liu, S.; Chen, J. *Dalton Trans.* **2009**, 1243–1250.
- (34) Lin, Y.; Yu, K.; Huang, S.; Liu, Y.; Wang, Y.; Liu, S.; Chen, J. *Dalton Trans.* **2009**, 9058–9067.
- (35) Axet, M. R.; Amoroso, F.; Bottari, G.; D'Amora, A.; Zangrando, E.; Faraone, F.; Drommi, D.; Saporita, M.; Carfagna, C.; Natanti, P.; Seraglia, R.; Milani, B. *Organometallics* **2009**, *28*, 4464–4474.
- (36) Ma, J.; Wang, L.; Zhang, W.; Zhou, Q. *Tetrahedron: Asymmetry* **2001**, *12*, 2801–2804.
- (37) Zai, S.; Liu, F.; Gao, H.; Li, C.; Zhou, G.; Cheng, S.; Guo, L.; Zhang, L.; Zhu, F.; Wu, Q. *Chem. Commun.* **2010**, *46*, 4321–4323.
- (38) Bianchini, C.; Gatteschi, D.; Giambastiani, G.; Rios, I. G.; Ienco, A.; Laschi, F.; Mealli, C.; Meli, A.; Sorace, L.; Toti, A.; Vizza, F. *Organometallics* **2007**, *26*, 726–739.
- (39) Benito, J. M.; de Jesús, E.; de la Mata, F. J.; Flores, J. C.; Gómez, R.; Gómez-Sal, P. *Organometallics* **2006**, *25*, 3876–3887.
- (40) Wang, C.; Friedrich, S.; Younkin, T. R.; Li, R. T.; Grubbs, R. H.; Bansleben, D. A.; Day, M. W. *Organometallics* **1998**, *17*, 3149–3151.
- (41) Laine, T. V.; Lappalainen, K.; Liimatta, J.; Aitola, E.; Lofgren, B.; Leskela, M. *Macromol. Rapid Commun.* **1999**, *20*, 487–491.
- (42) Laine, T. V.; Piironen, U.; Lappalainen, K.; Klinga, M.; Aitola, E.; Leskela, M. *J. Organomet. Chem.* **2000**, *606*, 112–124.
- (43) Irrgang, T.; Keller, S.; Maisel, H.; Kretschmer, W.; Kempe, R. *Eur. J. Inorg. Chem.* **2007**, 4221–4228.
- (44) McCord, E. F.; McLain, S. J.; Nelson, L. T. J.; Ittel, S. D.; Tempel, D.; Killian, C. M.; Johnson, L. K.; Brookhart, M. *Macromolecules* **2007**, *40*, 410–420.
- (45) Cotts, P. M.; Guan, Z.; McCord, E.; McLain, S. *Macromolecules* **2000**, *33*, 6945–6952.
- (46) Gao, H.; Pan, J.; Guo, L.; Xiao, D.; Wu, Q. *Polymer* **2011**, *52*, 130–137.
- (47) Gao, H.; Liu, X.; Tang, Y.; Pan, J.; Wu, Q. *Polym. Chem.* **2011**, *2*, 1398–1403.
- (48) Gottfried, A. C.; Brookhart, M. *Macromolecules* **2001**, *34*, 1140–1142.
- (49) Gottfried, A. C.; Brookhart, M. *Macromolecules* **2003**, *36*, 3085–3100.
- (50) Zhang, K.; Ye, Z.; Subramanian, R. *Macromolecules* **2008**, *41*, 640–649.
- (51) Zhang, Y.; Ye, Z. *Chem. Commun.* **2008**, 1178–1180.
- (52) McGuinness, D. S.; Brown, D. B.; Tooze, R. P.; Hess, F. M.; Dixon, J. T.; Slawin, A. M. Z. *Organometallics* **2006**, *25*, 3605–3610.
- (53) Lambertia, M.; Bortoluzzib, M.; Paoluccib, G.; Pellicchia, C. *J. Mol. Catal. A: Chem.* **2011**, *351*, 112–119.